"STUDY OF COMBUSTION MECHANISM OF NEW POLYMER/OXIDIZER MIXTURES"

Final Technical Report
by
Anatoli A. Zenin

May, 2002

United States Army

EUROPEAN RESEARCH OFFICE OF THE U.S.ARMY

London, England

CONTRACT NUMBER N68171-01-M-5482

R&D 8042-AN-01

Russian Academy of Sciences,
Semenov Institute of Chemical Physics

Approved for Public Release; distribution unlimited

REPORT DOCUMENTATION PAGE			Form Approved OMB No. 0704-0188
1. AGENCY USE ONLY	2. REPORT DATE 15 May 2002	3. REPORT TYPE AND DATES COVERED Final Report: 15 March 2001-15 May 2002	
4. TITLE AND SUBTITLE **"Study of Combustion Mechanism of New Polymer/Oxidizer Mixtures"**			5. FUNDING NUMBERS C
6. AUTHOR **Anatoli A. Zenin**			
7. PERFORMING ORGANISATION NAME AND ADDRESS Semenov Institute of Chemical Physics, Russian Academy of Sciences Kosygin Street 4, 119991 Moscow, Russia			8.PERFORMING ORGANISATION REPORT NUMBER -
9. SPONSORING/MONITORING AGENCY NAME AND ADDRESS **U.S. Naval Regional Contracting Center, Det. London,** **Government Buildings, Block 2, Wing 12,** **Lime Grove, Ruislip, Middlesex HA4 8BS, United Kingdom** **Tel 44 (0) 208-385-5311, Email t.mckamey@post.nctsl.navy.mil**			10. SPONSORING/MONITORING AGENCY REPORT NUMBER
11. SUPPLEMENTARY NOTES			
12a. DISTRIBUTION/AVAILABILITY STATEMENT			12b. DISTRIBUTION CODE

13. ABSTRACT

Combustion mechanisms of mixtures of CL-20 (hexanitrohexaazaisowurtzitane, or, HNIW) with active binder, plastified polyurethane (PUNE), 70:30, were investigated simultaneously with those of mixtures of PUNE/HMX, 30/70. Temperature profile and surface temperatures in combustion waves of the mixtures were measured at pressures 0.1-10 MPa and sample temperatures -100, 20 and 90°C. Burning rates, heat release in solid, heat feedback from gas to solid, heat release rate in gas, zone temperatures and sizes, macrokinetics of gasification, leading stages, sensitivities, criteria of stable combustion and response functions - were found. Conclusions about peculiarities of combustion mechanisms of the mixtures are presented. Recommendations for future works were formulated. Preliminary results for mixtures of (BAMO-AMMO)/CL-20, 20/80, were obtained.

14. SUBJECT ITEMS	15. NUMBER OF PAGES
CL-20, active binders, propellant mixtures, burning rates, temperature profiles, parameters of burning wave structure, macrokinetics, sensitivities, response functions, distinctions between combustion mechanisms.	22
	16. PRICE CODE NTIS

17. SECURITY CLASSIFICATION OF REPORT	18. SECURITY CLASSIFICATION OF THIS PAGE	19 SECURITY CLASSIFICATION OF ABSTRACT	20. LIMITATION OF ABSTRACT
UNCLASSIFIED	UNCLASSIFIED	UNCLASSIFIED	UL

Body of the Report

1. Background and Content of the Work

Mixtures of polymer binders with new oxidizers offer many advantages for advanced propulsions. Energetic binders are preferable for that propulsions. The study of combustion mechanisms of the energetic polymer binders/new oxidizers mixtures is important, because understanding of the mechanisms is useful for many applications of these propulsions. Temperature profiles of combustion waves were determined for mixtures with new oxidizer CL-20 (HNIW) and with HMX (70% of oxidizer). Active binder PUNE (plastified polyurethane rubber) was used. The work was performed at pressures 0.1-10 MPa and sample temperatures from -100 up to +90°C. Burning wave parameters were found by experiments and by processing of the experimental data. Deep processing of experimental data allows macrokinetics of gasification, leading stages, criteria of stable combustion, and sesitivities of burning rate and surface temperature to be established. Burn-rate response functions to oscillatory pressure were estimated. Preliminary results for advances mixtures (AMMO-BAMO)/HNIW, 20:80, are indicated.

2. Approach and Object of Investigations.

The following propellant mixtures were investigated:

1. PUNE/HNIW, 30:70, ρ=1,67 g/cm^3; sum formula: $O_{28.77}H_{24.095}N_{21.62}C_{17.697}$;
   T_{ad}=3171 K (at 10 MPa);
2. PUNE/HMX, 30:70, ρ=1,7 g/cm^3; sum formula: $O_{28.51}H_{33.42}N_{21.36}C_{17.566}$;
   T_{ad}=2717 K (at 10 MPa);

The used binder PUNE is a polyurethane rubber (PU), plastified by mixture of two nitroesters (NE): dinitratdietileneglycole and dinitrattrietilenglicole. Relation of PU:NE is 20:80 by weight. Polyurethane rubber has sum formula: $C_{48.1}H_{67.67}O_{20.1}N_{2.3}$. PUNE is an active binder, partly, due to large amount of nitroesters. Oxidizer HNIW (2,4,6,8,10,12-hexanitrohexaazaisowurtzitane), or CL-20, was a powder with cristal particles of rectangular shape of 5x3x3 μm in sizes. Employment of binder PUNE with oxidizer HNIW allowed propellant samples having high density, homogenity and high mechanical properties to be prepared.

Mixture PUNE:HMX, 30:70, with high density, homogenity and mechanical properties was prepared to compare combustion mechanisms of mixtures PUNE/HNIW and PUNE/HMX.

3. Experimental Techniques.

3.1. Conditions of experiments and microthermocouple techniques.

Temperature profiles of the combustion waves and the burning surface temperatures were obtained by microthermocouple methods. Profiles of the combustion waves were obtained by microthermocouples imbedded into solid. Thermocouples went through combustion waves when the waves propagated through the solid samples and show temperature profiles. The ribbon U-shaped thermocouples made of alloys W+5%Re/W+20%Re of 2-7 μm thick were imbedded into the samples. Cylindrical samples of 8 mm in diameter and 3 cm in length were cat by small thin knife of U-shape form, thermocouple placed into the created cross-sections, which were moistend by acetone, and the joined sections with thermocouples inside were protected by thin layer of polymer glue. Sample drying was performed during 6 ours. Every sample had inside 2-3 thermocouples placed one above the other. Distances between the junctions were 2-4 mm. The samples were burned in a bomb of constant pressure in atmosphere of nitrogen at pressures 0.1-10 MPa and at sample initial temperatures T_o= -100, +20, and +90°C. In experiments at different sample temperatures, the samples were placed into a small thermostat inside the bomb. Heating of

samples was made by electrically heated wires and cooling was performed by liquid nitrogen. The sample temperature was controlled by thermocouples. Samples were ignited by electrically heated wire. Thermocouple signals were registered by amplifier and oscillograph. Burning rate was measured by time delay between the thermocouple signals, by photoregistrations of sample combustion and by pressure increase during the sample combustion. Photoregistration of sample combustion allows also the type of combustion to be established. Burning surface temperatures were measured by thermocouples that are being pressed to the surface during sample combustion and by establishing the locations of slope breaks on temperature profiles registered by thermocouples (see below).

3.2. Temperature profile measurement validations. As a rule, temperature gradient close to the burning surface has a very high value. It implies that thermocouple measurements can give temperature profiles with significant errors due to thermocouple heat inertia. Because of that it is necessary to find conditions under which thermocouple measurements in combustion waves will introduce small errors. These conditions have been found by numerical simulations. The thermocouple partially absorbs the heat of the thermal layer and decreases the temperature at the point of the measurement. The requirement of small temperature error (less than 10%) of the thermocouple is indicated by the following formula: $h<0.2\ \chi/r_b$;

Here: h - thermocouple thickness (in cm), χ- heat diffusivity of the solid (in cm^2/s), r_b - linear burning rate (in cm/s). $\chi/r_b=l$ where l is the thickness of heat layer of the condensed phase. The thermocouples have to have U-shape form. It is necessary because of a high difference between heat conduction coefficients of metallic thermocouple wire and that of solid or gas. Junctions of U-shaped thermocouples do not experience large temperature decrease. Modelling experiments and numerical simulations show that the decrease of junction temperature will be small ($\leq 3\%$) if the horizontal part of the U-shaped thermocouple is about one hundred times more than thermocouple thickness h. Thermal inertia of the thermocouple in the gas phase can be taken into consideration and eliminated by a correction procedure. The procedure implies the use of the following equation:

$$dT_{ex}/dx=(r_b\tau_o)^{-1}\cdot(T - T_{ex});$$

Here: T - the real temperature of gas in the combustion wave; T_{ex} - the temperature registrated by thermocouple; τ_o - time response of the thermocouple in gas. Time response depends on mass burning rate m ($m=\rho\cdot r_b$) and temperature T. The temperature profiles in gas were corrected by this equation. The theory of thermocouple measurements in combustion waves of solids was created and confirmed by measurements of combustion wave temperature profiles by thermocouples with sequentially decreased thickness (method of "zero diameter"). All the above mentioned requirements have been met in the investigations. Different types of metal wires for thermocouples were used (We,Re and Pt,Rh) to test the catalytic effect on thermocouples. The catalytic effect was not observed. The method of burning surface temperature measurement by determining locations of slope breaks on temperature profiles registered by thermocouples (method of "slope break") is based on the existence of the horizontal delay of value ($r_b\tau_o$) on the temperature profiles when thermocouples go through the burning surface. The delay is due to the change of heat exchange between environment and thermocouple: contact heat exchange in solid is replaced by convective heat exchange in gas.

4. Results of Measurements and Processing

The prepared mixtures No.1 (PUNE/HNIW) and No.2 (PUNE/HMX) were studied in this work detailed at sample temperatures T_o= - 100, 20 and +90°C. Uniform contents of the mixtures allow decreased scattering of all combustion characteristics to be obtained. The samples have density ρ=1,67 g/cm^3 for mixture No.1 and ρ=1,7 g/cm^3 for mixture No.2. The thermodynamic

calculated adiabatic flame temperatures T_{ad} are equal to 3171 K (at 10 MPa) and 2717 K (at 10 MPa), correspondingly.

Mixture 1 and mixture 2 burn at T_o= 20 and +90°C, relatively steady, without periodically pulsations of burning rate. Burning waves have stable propagation at these T_o in samples of mixture 1 beginning from 0.1 MPa, but in samples of mixture 2 it takes place only beginning from 0.25 MPa. At T_o= - 100°C the samples of mixture 1 burn steady, beginning from p> 1 MPa and mixture 2 - beginning from p= 1 MPa. Both mixtures burn relatively steady up to 10 MPa.

Carbon residue. A significant carbon residue produces on the burning surface of mixture 1 at decreased pressures. This residue approximately holds the shape of the sample after going of the burning wave at pressures 0.1-1.5 MPa. At higher pressures the carbon residue has forms of carbon flakes which accumulale on walls of the bomb. The mean density of the residue ρ_{cb} is low: ρ_{cb} = 0.01 - 0.02 g/cm^3. Only quite close to the burning surface a thin layer of relatively dense carbon residue with $\rho_{cb} \approx 0.1$ g/cm^3 is observed (however, probably, this layer produces only during the sample extinguishing). There is not influence of T_o on the carbon residue production. The residue, which holds the shape of sample, is a carbon lattice, through which gaseous combustion products blow. These gases are a good electrical insulater and because of that the thermocouple signal don't have any distortions when thermocouple is in the gas phase of the combustion waves at low pressures.

Carbon residue on the burning surface of mixture 2 did not observed.

Temperature profiles. Figures 1 - 12 present obtained averaged temperature profiles T(x), in solid and gas, for mixtures 1 and 2 at different pressures and sample temperatures. Figures 1, 3, 5, 7, 9, and 11 present averaged distributions of temperature T(x) along the burning waves of mixture 1 at 0.1-10 MPa and different T_o. Figures 2 - 12 (even numbers) present the distributions for mixture 2 at 0.25 - 10 MPa. The figures show that both mixtures have temperature profiles T(x) with similar features: at 0.1-0.25 MPa the temperature profiles have only low-temperature (first) zone in the gas phase, at 0.5 MPa flame zone evolve into existence and at 1.0 MPa the flame zone acquires more high temperature. At 2 MPa two-zone sructure still exists, but at 5-10 MPa both zone merge into one zone of the gas phase.

Temperature profiles of mixture 1 have significant temperature pulsations in the gas phase at T_o= - 100°C and pressure 1 MPa. Pressure increasing significantly decreases amplitude of the temperature pulsations at T_o= - 100°C. At T_o= 20 and 90°C the temperature profiles relatively smooth in pressure interval 0.1-10 MPa. Only at pressures close to 2 MPa, increased temperature pulsations in the gas phase are observed at the investigated T_o. A possible explanation of the phenomenon is as follows: it takes place due to carbon flakes tearing off from the burning surface. Indeed, going of that flakes close to the thermocouple junction have to cause a local temperature rising (carbon lattice catalize gas reactions and because of that the gas close to the lattice have an increased temperature). At p>2 MPa amount of flakes decreases and, possibly, because of that amplitudes of temperature pulsations on temperature profiles decrease.

Temperature profiles of mixture 2 at all investigated pressures and initial temperatures have only small irregular pulsations, which are typical for many propellant mixtures.

Processing of the obtained temperature profiles allow burning wave parameters to be determined. Tables 1 and 2 present dependencies of the parameters on pressure at various T_o for mixture 1. Tables 3 and 4 present the parameters for mixture 2.

Mass burning rates m. It can be seen from Tables 1-4 that burning rates of mixture 1 are significantly higher than the rates of mixture 2. Indeed the burning rates of mixture 1 at T_o= 20°C in pressure interval 0.1-10 MPa comprise 0.22-2.34 g/cm^{2}c, but those of mixture 2 in pressure interval 0.25-10 MPa comprise 0.05- 0.87 g/cm^{2}c. Similar result is observed at other initial temperatures. Indeed, at T_o= 90°C values of m of mixture 1 comprise 0.28-2.78 g/cm^{2}c (0.1-10

MPa), but for mixture 2 - 0.08 1.05 g/cm^{2}c (0.25-10 MPa). At T_o= -100°C m of mixture 1 comprise 0.3-2.12 g/cm^{2}c (1-10 MPa), but for mixture 2 - 0.12 0.72 g/cm^{2}c (1-10 MPa).
Standard deviation of m measurements is ±5 %.

Burning surface temperatures T_s. It can be seen from Tables 1-4 that burning surface temperatures T_s of mixture 1 significantly lower than surface temperatures of mixture 2. Indeed the surface temperatures of mixture 1 at T_o= 20°C comprise 235-318°C (0.1 - 10 MPa), but those of mixture 2 comprise 308-470°C (0.25-10 MPa). It can be seen also that surface temperature of mixture 1 increases slowly than that of mixture 2 in the studied pressure interval. Similar results are observed at other initial temperatures. Indeed, at T_o= 90°C T_s of mixture 1 comprise 243-326°C (0.1-10 MPa), but those of mixture 2 comprise 320-480°C (0.25-10 MPa). At T_o= -100°C T_s of mixture 1 comprise 240-312°C (1-10 MPa), but those of mixture 2 comprise 330-455°C (1-10 MPa). Standard deviation of T_s measurements is about ±5 %.

Geometric and temperature characteristics of temperature profiles in gas.

As it was mentioned above, the gas phase of the burning waves of the studied mixtures has two type of the structure: single-zone and two-zone structures. The mixtures always have two-zone structure at p=0.5-2.0 MPa and both zones merge at p≥5.0 MPa. At 0.1 -0.25 MPa only the first flame exists. Values of mean temperature of the first flame T_1 at T_o= 20°C for mixture 1 are equal to 900-1050°C (0.1-2 MPa) and for mixture 2 - 850-1100°C (0.25-2 MPa). When initial temperature changes, values of T_1 changes by similar way. So, at T_o= 90°C values of T_1 are equal to 950-1100°C (0.1-2 MPa) and for mixture 2 - 1000-1150°C (0.25-2 MPa). At T_o= -100°C values of T_1 for mixture 1 are equal to 800-900°C (1-2 MPa) and for mixture 2 - 950-1000°C (1-2 MPa). Standard deviation of T_1 measurements is ±10 %.

Flame temperatures T_f at T_o= 20°C for mixture 1 are equal to 1600-2860°C and for mixture 2 - 2200-2485°C. When initial temperature changes, values of T_f also changes by similar way. So, at T_o= 90°C values of T_f for mixture 1 are equal to 1700-2900°C (0.5-10 MPa) and for mixture 2 - 2250-2500°C (0.5-10 MPa). At T_o= -100°C values of T_f for mixture 1 are equal to 2200-2760°C (1-10 MPa) and for mixture 2 - 2150-2330°C (1-10 MPa).

Maximal flame temperatures T_f are obtained at 5 MPa for both mixtures at all T_o.

Distances L_1 between the burning surface and the beginning of the flame zone decrease when pressure increases. In fact, L_1 is the length of the first flame. Values of L_1 at T_o= 20°C are equal to 2- 0.4 mm for mixture 1 (0.1-2 MPa) and to 1.3-0.25 mm for mixture 2 (0.25-2 MPa). Increasing T_o increases L_1 and decreasing T_o decreases L_1 for both mixtures. So, at T_o= 90°C values of L_1 for mixture 1 are equal to 2.5-0.6 mm (0.1-2 MPa) and for mixture 2 - 1.5-0.3 mm (0.25-2 MPa). At T_o= -100°C values of L_1 for mixture 1 are equal to 0.4-0.3 mm (1-2 MPa) and for mixture 2 - 0.4-0.2 mm (1-2 MPa). The obtained data show that the first flame is an induction zone for both mixtures.

Distances L between the burning surface and the flame (up to 0.99 T_f) also decrease when pressure increases. In fact, L is the length of the gas phase reaction zone. Values of L at T_o= 20°C are equal to 2.5-1.5 mm for mixture 1 (0.5-10 MPa) and 2.8-0.7 mm for mixture 2 (0.5-10 MPa). Increasing T_o also increases L and decreasing T_o decreases L for both mixtures. So, at T_o= 90°C values of L for mixture 1 are equal to 3-1.2 mm (0.5-10 MPa) and for mixture 2 - 3-1 mm (0.5-10 MPa). At T_o= -100°C values of L for mixture 1 are equal to 3-1.5 mm (1-10 MPa) and for mixture 2 - 2.5-0.6 mm (1-10 MPa).

Standard deviations of L_1 and L measurements are ±15 %.

Coefficients of heat diffusivity and heat conductivity in solid heat layer.

Coefficients of solid heat diffusivity were obtained by formula $\chi = l \cdot r_b$, where l is thickness of heat layer of the condensed phase (see next section). Tables 1-4 show that values of χ increase when pressure increases. Values of χ are independent on T_o and increase when mean solid heat layer

temperature increases. The values for mixture 1 are equal to $(1.0\text{-}1.1)\cdot10^{-3}$ cm^2/s at 0.1 MPa and increase up to $(2.7\text{-}3.0)\cdot10^{-3}$ cm^2/s at 10 MPa. For mixture 2 χ comprise $(0.8\text{-}1.0)\cdot10^{-3}$ cm^2/s at 0.1 MPa and $(2.2\text{-}2.5)\cdot10^{-3}$ cm^2/s at 10 MPa. These values are typical ones for χ of solid heat layer of many propellant mixtures.

The coefficients of solid heat conduction were obtained by formula $\lambda_s=\chi\cdot c\cdot\rho$. It was assumed that solid specific heat is equal to $c=0.35$ cal/g·K for mixture 1 and $c=0.33$ cal/g·K for mixture 2 (these values of c were obtained by calculations of theory of solids). Tables 1-4 show that λ_s increases with pressure, is independent, practically, on T_o and also increases when mean solid heat layer temperature increases. Values of λ_s comprise $(5.8\text{-}17)\cdot10^{-4}$ cal/cm·s·K for mixture 1 and $(4.5\text{-}14)\cdot10^{-4}$ cal/cm·s·K for mixture 2. These values are also typical ones for λ_s of solid heat layer of many propellant mixtures.

Characteristic sizes in gas and solid.

Characteristic thickness l and l_m in solid (values of l_m was detemined only for mixture 2), presented on Tables 1-4, were obtained by temperature distributions in the condensed phase. Experimentally obtained thickness of heat layer in solid l is a distance between the burning surface and a section in solid with temperature $T^*=(T_s-T_o)/e - T_o$ (e is the base of ln). Thickness of l_m of the partly melt layer (with melt HMX) in the condensed phase is a distance between the burning surface and a section with HMX's melt temperature $T_m=280°C$. Tables show that thickness of l and l_m decrease when pressure increases. Values of l_m are less than values of l.

Conductive sizes ϑ of the gas phase were obtained by formula: $\vartheta=\lambda_g/mc_p$; where λ_g is coefficient of heat conduction in gas and c_p is coefficient of specific heat of the gas phase. Values λ_g and c_p were estimated by content of combustion products. The obtained dependencies of $\lambda_g(T_s)$ and $c_p(T_s)$ are presented on Table 5. Tables 1-4 show that values of ϑ decrease when pressure increases. Values of ϑ comprise 32-3 μm for mixture 1 and 102-6.7 μm for mixture 2. It can be seen that always $\vartheta<<L_1$ and $\vartheta<<L$.

Relative thickness of the gas-phase reaction layer were estimated by formula $\Omega=L_1/\vartheta$ at $p\le2$ MPa, and by formula $\Omega=L/\vartheta$ at $p>2$ MPa. It can be seen from Tables 1-4 that inequality of $\Omega>>1$ always takes placee. It implies that a wide reaction zone in the gas phase is observed for all combustion regimes of both mixtures.

Heat manifestations: heat release in solid and heat feedback from gas into solid.

The temperature profiles and burning surface temperatures were used for obtaining heat parameters of the burning waves. Heat flux from gas to solid $q\cdot m$ by heat conduction can be estimated by the following formula: $q\cdot m=-\lambda_g(T)\cdot(dT/dx)_o$;

Here: $(dT/dx)_o=\varphi$ is the temperature gradient in gas close to the burning surface.

Heat feedback q from gas into solid by heat conduction can be estimated by the following formula:

$$q=-\lambda_g(T)\cdot\varphi/m;$$

Formula for heat release Q in reaction layer of the condensed phase (or on the burning surface) for mixture 1 has the following form:

$$Q=c\cdot(T_s-T_o)-q-q_r;$$

Formula for heat release Q for mixture 2 is as follows:

$$Q=c\cdot(T_s-T_o)-q-q_r+q_m;$$

where q_m is the heat of HMX melting in mixture 2; temperature of HNIW's melting and heat of HNIW's melting are not known and because of that formula for mixture 1 doesn't have member of q_m. Heat of HMX's melting is equal to 24 cal/g (per gramm of HMX) and because of that $q_m=16.8$ cal/g (per gramm of mixture 2). Radiant heat feedback q_r from flame into solid was estimated for both mixtures by using content of combustion products and real flame thick of the burning samples in our bomb of constant pressure. The heat radiations of CO_2, H_2O, H_2, etc were

taken into considerations. It was assumed that coefficient of heat radiation absorbtion of the burning surface was equal to 0.5. Tables 1-4 show the obtained heat parameters.

Mixture 1. It can be seen from Tables 1-2 that mixture 1 has significant positive heat release in solid. Values of Q comprise at pressures 0.1-10 MPa: 47-90 cal/g at T_0= 20°C and 28-67 cal/g at T_0= +90°C. At pressures 1-10 MPa and T_0= -100°C values of Q are elevated and comprise 91-132 cal/g. Parameter Q increases always with pressure. It can be seen also that temperature gradient φ in gas close to burning surface has significant values and always increases with pressure. Parameter φ comprise in the studied pressure intervals values of $(3\text{-}17)\cdot10^{-4}$ K/cm at T_0= 20°C, $(3.5\text{-}15)\cdot10^{-4}$ K/cm at T_0= 90°C and $(5.5\text{-}20)\cdot10^{-4}$ K/cm at T_0= -100°C. On the contrary, heat feedback q from gas into solid decreases always when pressure increases. Values of q are comparable with values of Q only at low pressures and at T_0= +90°C. Under other conditions values of q significantly lowere than Q. Indeed, Tables 1-2 show that q comprises in the studied pressure intervals 27-15, 25-10 and 31-11 cal/g at T_0= 20, 90 and -100°C, correspondingly.

Mixture 2. It can be seen from Tables 3-4 that mixture 2 has typical burning wave parameters for nitramine containing compositions. Partly, the tables show that values of Q are large and values of q are relatively low.

Table 1: Burning wave parameters of mixture 1 (PUNE/HNIW) at T_0=20°C.

N	p, MPa	0.1	0.5	1.0	2.0	5.0	8.0	10.0
1	m, g/cm²s	0.22	0.43	0.62	0.92	1.58	2.06	2.34
2	T_s, °C	235	257	268	285	304	314	318
3	$\varphi\cdot10^{-4}$, K/cm	3.0	5.5	7.5	9	12.5	15	17
4	q, cal/g	27	26	24	18	16	15	16
5	q_r, cal/g	0.8	0.5	3.1	3.3	4.3	4.8	4.8
6	Q, cal/g	47	57	59	72	79	83	90
7	l, μm	78	50	40	35	25	22	22
8	$\chi\cdot10^3$, cm²/s	1.0	1.3	1.5	2.0	2.4	2.6	2.8
9	$\lambda_s\cdot10^4$, cal/cm·s·K	5.8	7.5	8.7	11.6	14	15	16
10	T_1, °C	900	950	1000	1050	-	-	-
11	T_f, °C	-	1600	2300	2500	2860	2860	2860
12	L_1, mm	2.0	1.2	0.6	0.4	-	-	-
13	L, mm	-	2.5	3.0	2.0	2.5	2.0	1.5
14	ϑ, μm	32	17	12	9.5	5.4	4.4	4.0
15	Ω	63	70	50	42	460	450	375
16	Φ_o, kcal/cm³s	2.4	8.8	17.2	30.6	70.3	114	147

Table 2: Burning wave parameters of mixture 1 (PUNE/HNIW) at T_o=+90 and -100°C (+90 °C/-100°C)

N	p, MPa	0.1	0.5	1.0	2.0	5.0	8.0	10.0
1	m, g/cm²s	0.28/-	0.54/-	0.8/0.3	1.2/0.52	1.98/1.18	2.5/1.78	2.78/2.12
2	T_s, °C	243/-	265/-	276/240	293/260	312/295	322/308	326/313
3	$\varphi \cdot 10^{-4}$, K/cm	3.5/-	4.5/-	6.5/5.5	8/7	11/12	13/17	15/20
4	q, cal/g	25/-	17/-	16/31	13/23	11/18	10/17	11/17
5	q_r, cal/g	0.8/-	0.5/-	3.1/3.1	3.3/3.3	4.3/4.3	4.8/4.8	4.8/4.8
6	Q, cal/g	28/-	44/-	46/91	55/100	62/116	66/121	67/132
7	l, μm	65/-	43/-	34/80	30/60	22/35	19/25	18/23
8	$\chi \cdot 10^3$, cm²/s	1.1/-	1.4/-	1.6/1.4	2.2/1.9	2.6/2.4	2.8/2.5	3.0/2.7
9	$\lambda_s \cdot 10^4$, cal/cm·s·K	6.3/-	8.0/-	9.3/8.2	12.7/11	15/14	16/14.6	17/15.8
10	T_l, °C	950/-	1000/-	1050/800	1100/900	-/-	-/-	-/-
11	T_f, °C	-/-	1700/-	2400/2200	2600/2400	2900/2760	2900/2760	2900/2760
12	L_1, mm	2.5/-	1.8/-	1.3/0.4	0.6/0.3	-/-	-/-	-/-
13	L, mm	-/-	3/-	3.5/3	2.5/2.2	2.5/2.5	1.8/2.2	1.2/1.5
14	ϑ, μm	26/-	14/-	9.6/24.8	6.4/13.8	4.0/6.8	3.2/4.8	3.0/4.1
15	Ω	96/-	128/-	135/16	94/22	625/368	560/458	400/366
16	Φ_o, kcal/cm³s	3.6/-	9.0/-	19.2/6.2	35.5/13.5	80.6/52.4	120/112	154/157

Heat release rate in gas close to the burning surface.

Heat release rates Φ_o in gas close to the surface were estimated by the use of the obtained data. Φ_o shows, obviously, the intensity of chemical reactions in gas. Values of Φ_o were obtained by the following expression: $\Phi_o = c_p \cdot m \cdot \varphi$;

Values of c_p were taken at 500°C. Tables 1-4 show that values of Φ_o quickly increase with pressure. Mixture 1 has in the studied pressure intervals the following values of Φ_o:

2.4-147 kcal/cm³s at T_0= 20°C, 3.6-154 kcal/cm³s at T_0= 90°C and 6.2-157 kcal/cm³s at T_0= -100°C. Mixture 2 has in the studied pressure intervals the following values of Φ_o:

0.28-56 kcal/cm³s at T_0= 20°C, 0.64-80 kcal/cm³s at T_0= 90°C and 1.2-43 kcal/cm³s at T_0= -100°C. Thus mixture 1 has more intensive chemical reactions in gas near the burning surface than mixture 2.

Table 3: Burning wave parameters of mixture 2 (PUNE/HMX) at T_o=20°C.

No	p, MPa	0.25	0.5	1.0	2.0	5.0	8.0	10.0
1	m, g/cm^{2}s	0.05	0.084	0.16	0.29	0.57	0.76	0.87
2	T_s, °C	308	322	242	382	435	460	470
3	$\varphi \cdot 10^{-4}$, K/cm	1.4	2.1	3.0	5.0	10	14	16
4	q, cal/g	50	45	34	30	32	32	34
5	q_r, cal/g	0.5	4.4	3.9	3.7	3.3	2.5	2.6
6	Q, cal/g	62	67	86	102	122	128	128
7	l, μm	270	220	140	90	60	50	50
8	l_m, μm	40	35	30	25	25	22	20
9	$\chi \cdot 10^3$, cm^2/s	0.8	1.1	1.3	1.6	2.0	2.3	2.5
10	$\lambda_s \cdot 10^4$, cal/cm·s·K	4.5	6.2	7.3	9.0	11	13	14
11	T_1, °C	850	1000	1050	1100	-	-	-
12	T_f, °C	-	2200	2250	2400	2435	2435	2435
13	L_1, mm	1.3	0.9	0.5	0.25	-	-	-
14	L, mm	-	2.8	1.8	2.0	1.3	1.0	0.7
15	ϑ, μm	102	68	37	21	12	9	8
16	Ω	13	13	14	12	108	110	88
17	Φ_o, kcal/cm^{3}s	0.28	0.7	1.9	5.8	22.8	42.6	56

Table 4: Burning wave parameters of mixture 2 (PUNE/HMX) at T_o=+90 and -100°C (+90 °C/-100°C)

N	p, MPa	0.25	0.5	1.0	2.0	5.0	8.0	10.0
1	m, g/cm²s	0.08/-	0.14/-	0.21/0.12	0.36/0.2	0.7/0.43	0.94/0.62	1.05/0.72
2	T_s, °C	320/-	340/-	360/330	400/360	450/412	473/440	480/455
3	$\varphi \cdot 10^{-4}$, K/cm	2/-	3/-	4.5/2.5	7/4	13/9	17/13	19/15
4	q, cal/g	45/-	39/-	39/31	38/32	33/34	33/34	33/36
5	q_r, cal/g	0.6/-	3.1/-	3.5/4	3.0/4	2.9/3.5	2.4/2.7	2.3/2.7
6	Q, cal/g	47/-	58/-	64/124	76/133	99/148	108/158	111/161
7	l, μm	210/-	140/-	100/170	65/120	45/65	40/55	40/50
8	l_m, μm	40/-	35/-	30/25	25/30	25/22	25/20	25/20
9	$\chi \cdot 10^3$, cm²/s	1.0/-	1.1/-	1.2/1.2	1.4/1.4	1.8/1.6	2.2/2.0	2.5/2.2
10	$\lambda_s \cdot 10^4$, cal/cm·s·K	5.6/-	6.2/-	6.7/6.7	7.8/7.8	10/9.0	12/11.2	14/12.3
11	T_1, °C	1000/-	1050/-	1100/950	1150/1000	-/-	-/-	-/-
12	T_f, °C	-/-	2250/-	2300/2150	2450/2300	2500/2330	2500/2330	2500/2330
13	L_1, mm	1.5/-	1.2/-	0.6/0.4	0.3/0.2	-/-	-/-	-/-
14	L, mm	-/-	3/-	2/2.5	2.5/2.3	2/1.2	1.2/1.0	1/0.6
15	ϑ, μm	71/-	42/-	29/45.6	18/28.6	10/15	7.5/10.5	6.7/9
16	Ω	21/-	29/-	20/8.8	17/7.0	200/80	160/95	150/67
17	Φ_o, kcal/cm³s	0.64/-	1.7/-	3.7/1.2	10/3.2	36/15.5	64/32	80/43

Table 5: Coefficients of heat conduction λ_g and specific heat c_p of the gas phase

mixtures	T, °C	300	500	800	1000	1500
No. 1	$\lambda_g \cdot 10^4$, cal/cm·c·K	1.5	2.0	3.0	3.7	5.1
	c_p, cal/g·K	0.31	0.37	0.45	0.49	0.62
No. 2	$\lambda_g \cdot 10^4$, cal/cm·c·K	1.4	1.6	2.0	2.4	3.8
	c_p, cal/g·K	0.38	0.40	0.415	0.42	0.45

5. Deep Processing of Experimental Data

Burning Rate Control Regions.

The results of measurements of $q+q_r$ and Q and the investigations of the gas phase zone behaviour show that burning rate of mixtures 1, 2 are caused by the heat release in solid (or on solid surface) and, in a smaller degree, by the heat feedback from the gas layer which is close to the burning surface. It was mentioned above also that the values of of $q+q_r$ decreases when the burning rate increases. These facts show that heat release in solid (or on solid surface) is a main factor of creating burning rate in mixtures 1, 2. Heat feedback from gas to solid is only small additional factor of the burning rate creating and influence of this factor on values of m decreases when pressure increases (at pressures $p \leq 10$ MPa). Then, the obtained data, presented in Tables 1-5, allow an important conclusion to be made: the high temperature region of the burning waves cannot affect the burning rate. Indeed, the influence of the heat release in the gas phase on the burning rate can be estimated by the following formula obtained as a solution of the heat conduction equation:

$$m \cdot q = \int_0^\infty \Phi(x) \cdot \exp(-x/\vartheta) \cdot dx;$$

This formula shows that influence of heat release in gas (here $\Phi(x)$·is distribution of heat release rate in the gas phase) on m decreases very quickly when $x > \vartheta$. Tables 1-4 show that values ϑ are small and they are significantly smaller than gas zone sizes L and L_1. That implies that high temperature region of the burning waves cannot affect the burning rate.

Thus the obtained results show that the burning rate control regions in the combustion waves for all regimes of the mixtures combustion, under investigated conditions, are the regions of heat release in solid just under the burning surface (or immediately on the burning surface) and thin low-temperature gas layers close to the burning surface (at $x \approx \vartheta$). High temperature gas regions cannot influence the burning rate in fact because of a very large heat resistance of the gas phase of the mixtures.

Macrokinetics of Solid Gasification.

The following equation connects burning rate of solid with burn-surface temperature and macrokinetic characteristics of solid gasification:

$$m^2 = \lambda_s \rho / Q^2 \cdot \Re T_s^2 / E \cdot k_o Q^* \cdot 1/N \cdot \exp(-E/\Re T_s);$$

where $N = 1/\eta_s + (1-\eta_s)/\eta_s \cdot \ln(1-\eta_s) - (q/Q) \cdot [\ln(1-\eta_s)]/\eta_s$; $\eta_s = Q/Q^*$; Q^* is the maximum of the heat release in solid, E is activation energy of limiting stage of the gasification process, T_s in K. For studied combustion waves $N \cong 1$. The expression was obtained by solution of system of two equations for the steady propagated burning wave (were solved the heat conduction equation for solid phase and the equation of diffusion of reagents). The burning wave propagates due to heat release in solid Q and heat feedback from gas to solid q. Function of the volumetric heat release rate Φ_s in solid was assumed as follows:

$$\Phi_s(\eta, T) = Q^* k_o \cdot \rho \cdot (1-\eta) \cdot \exp(-E/\Re T);$$

Here η is the reaction completeness ($\eta = \eta_s$ on the burning surface), k_o is the preexponent multiplier.

The member $\exp(-E/\Re T_s)$ plays the most important role in this formula. Because of that the connection m and T_s can be presented by the following simplified expression:

$$m = A \cdot \exp(-E/2\Re T_s);$$

This expression has been designated "gasification law". The results of measurement, presented in Tables 1, 2, allow the following gasification law for mixture 1 to be obtained:

$$m=4.0\cdot10^6\cdot\exp(-34000/2\Re T_s);\quad (m \text{ in g/cm}^2\text{s},\ T_s \text{ in K})$$

Possibly, value E=34000 kcal/mole is an activation energy of the limiting stage of the process of oxidizer CL-20 gasification in the reaction layer of mixture 1.

The results of measurement, presented in Tables 3, 4, allow the following gasification laws for mixture 2 to be obtained:

$$m=3.8\cdot10^3\cdot\exp(-25000/2\Re T_s);\quad (m \text{ in g/cm}^2\text{s, T in K, at } T_s<470^\circ\text{C}),$$

The obtained value of activation energy of the gasification process is very close to that of cyclic nitramines (when $T_s<470^\circ$C). Possibly, gasification of oxidizer HMX in the reaction layer of burning mixture 2 is the limiting stage of the process of the mixture gasification.

Pressure and Temperature Sensitivities of burning rate and surface temperature.

The following pressure and temperature sensitivities for burning rate and burning surface temperature were found from the data presented on Tables 1-4:

$\beta=(\partial\ln m/\partial T_o)_{p\text{-const}}$, - temperature sensitivity of mass burning rate;

$r=(\partial T_s/\partial T_o)_{p\text{-const}}$, - temperature sensitivity of burning surface temperature;

$\nu=(\partial\ln m/\partial\ln p)_{T_o\text{-const}}$, - pressure sensitivity of mass burning rate;

$\mu=(T_s-T_o)^{-1}\cdot(\partial T_s/\partial\ln p)_{T_o\text{-const}}$, - pressure sensitivity of burning surface temperature;

The obtained results for mixtures 1 and 2 are shown on Tables 6 for $T_o=20^\circ$C. It can be seen that burn-rate pressure sensitivity ν for mixture 1 comprises 0.42-0.58, and in pressure interval 2-10 MPa $\nu=0.58$=const. This parameter for mixture 2 comprises 0.76-0.6. So, parameter ν for mixture 1 is significantly less than that for mixture 2. Burn-rate temperature sensitivity β of mixtures 1 is equal to $(0.48\text{-}0.19)\cdot10^{-2}$ 1/K and that of mixture 2 - $(0.3\text{-}0.2)\cdot10^{-2}$ 1/K. So, burn-rate temperature sensitivity of mixtures 1 is elevated, in comparison with that of mixture 2. Surface temperature sensitivity r of mixtures 1 (0.17-0.08) is less than r of mixture 2 (0.17-0.23-0.14). Parameter μ of mixture1 (0.064-0.088-0.064) also is less than μ of mixture 2 (0.072-0.166-0.103).

Criteria of Stable Combustion. Criterion of stable combustion - Zeldovich's criterion $k=\beta\cdot(T_s-T_o)$ - is presented also on Table 6. It can be seen that at pressures 0.25 - 2 MPa k can exceed unity. Novozilov's criterion $k^*=(k-1)^2/(k+1)r$ is necessary to calculate for regimes having values of $k>1$. Combustion is stable if $k^*<1$. Estimations of k^* show that mixtures 1 and 2 always have stable combustion at $T_o=20^\circ$C. This conclusion confirms results obtained for temperature profile measurements - see above n. 4.

Pressure-Driven Burn-Rate Response Functions.

The obtained results, which were received under conditions of constant, nonpulsating pressures, allow us to investigate burning rate behaviour of mixtures 1 and 2 under conditions of oscillatory pressure. It can be made due to found above sensitivities for m and T_s. This paragraph is devoted to these investigations. Let us assume that $p=p_o+p_1\cdot\cos\varpi t$, where $p_1<<p_o$ and ϖ is cyclic frequency of oscillation in 1/s. Then nondimensional burning rate is equal to $V=1+V_1\cdot\cos\varpi t$, where $V=r_b/r_{bo}$, $V_1=r_b^{\sim}/r_{bo}$; r_{bo} is a stationary burning rate and $r_b^{\sim}$ is a pulsating burning rate, which takes place due to pressure pulsations. It is convenient to analyse burning rate response in complex form. In this case complex nondimensional burning rate is equal to $V=1+V_1\cdot e^{-i\omega t}$ and complex nondimensional pressure is equal to $\eta=1+\eta_1\cdot e^{-i\omega t}$, where $\eta_1=p_1/p_o$, and ω is nondimensional frequency.

The following expression for burning rate response function to oscillatory pressure takes place:

$$U=[\nu+(\nu\cdot r-\mu\cdot k)\cdot(z-1)]/[1+r\cdot(z-1)-k\cdot(z-1)/z];$$

Here $z=(1+\sqrt{1+4i\omega})/2$; $U=V_1/\eta_1$, V_1 is nondimensional burning rate complex amplitude, and ω is nondimensional frequency which is equal to the cyclic frequency ϖ, in 1/s, multiplied by the time of solid heat layer relaxation χ/r_b^2. Values of ν, μ, k and r here are based on the mean pressure p_o and because of that data from Table 6 can be used for estimations of complex functions of U. Thus, indeed, we can investigate burning rate behaviour of mixtures 1, 2 under conditions of pulsating pressure.

Results of calculationsof dimensionless amplitudes Re{U}of burning rate pulsations and phase of the pulsations, Im{U}, as functions of ω are shown on Table 7. The used denominations are as follows:

$Re\{U\}_m$ is maximum of Re{U} (in the nondimensional frequency interval ω =0-20);

ω_{n1} - nondimensional frequency, corresponding to this maximum;

ω_{n2} - nondimensional frequency, corresponding to Im{U} =0;

$Re\{U\}_o = Re\{U(0)\}$;

$Re\{U\}_{20} = Re\{U(20)\}$;

$Im\{U_{m+}\}$ - maximum of Im{U} in interval ω =0-ω_{n2}, i.e. in positive region of values of ImU;

ω_{im1} - nondimensional frequency, corresponding to this maximum;

$Im\{U_{m-}\}$ - minimum of ImU (if this minimum takes place) in negative region of ImU;

ω_{im2} - nondimensional frequency, corresponding to this minimum;

ϖ_{n1} , ϖ_{n2} , ϖ_{im1} , ϖ_{im2} - corresponding cyclic frequencies, in 1/s.

Estimations show that resonance frequencies $\omega_{n1,2}$ are equal approximately to theoretical values $\omega_n=\sqrt{k}/r$. Typical response functions of Re{U} and Im{U} for mixtures 1 and 2 are shown on Figures 13, 14. It can be seen that response functions of mixtures 1 and 2 are relatively close each other. It is natural that function $Im\{U(\omega)\}$, presenting the phase of response functions, changes the sign at the resonance frequency. Functions of $Re\{U(\omega)\}$ weakly depend on ω, especially at elevated p. The result shows that resonance phenomena in burning the mixtures are significantly depressed due to viscous behaviour of the oscillations. In fact, the pulsating combustion of the mixtures is an example of a relatively smoothed resonance phenomenon.

It is necessary to indicate here same differences between response functions of mixture 1 and 2. Table 7 shows that maximal amplitude of the response $Re\{U\}_m$ of mixture 1 in frequence interval 0-20 comprises 1.1-1.5-0.85, and that of mixture 2 - 2.5-1.4-1.1. So, amplitude reactions on pressure pulsations for mixture 1 are less than that of mixture 2. Table 7 also shows that differences ($Re\{U\}_m$ - $Re\{U\}_{20}$), as a rule, are less for mixture 1, in comparison with that of mixture 2. Indeed, this value for mixture 1 is 0.6-0.7-0.1, but for mixture 2 - 0.8-0.6-0.5. It is important to stress also that differences ($Re\{U\}_{20}$ - $Re\{U\}_o$) are positive for mixture 1 and they are negative for mixture 2. Both these facts show that amplitude of response functions of mixture 1 have more viscous character than the amplitude of response functions of mixture 2.

It is a very important result obtained here - see Table 7 - that cyclic resonance frequencies ϖ_{n1} for mixture 1 approximately an order higher than cyclic resonance frequencies ϖ_{n2} for mixture 2.

Table 6: Sensitivities of burning rate and surface temperature of mixtures 1 and 2 to pressure and initial temperature (for T_o=20°C)

		pressure, MPa							
	property	0.1	0.25	0.5	1.0	2.0	5.0	8.0	10
mixt.1	ν	0.42		0.47	0.52	0.58	0.58	0.58	0.58
	r	0.18		0.18	0.17	0.15	0.10	0.08	0.08
	μ	0.064		0.06	0.08	0.09	0.09	0.08	0.06
	k	1.18		1.19	1.19	1.14	0.85	0.68	0.57
	$\beta \cdot 10^{-2}$, 1/K	0.55		0.50	0.48	0.43	0.30	0.23	0.19
mixt.2	ν		0.86	0.86	0.86	0.75	0.73	0.62	0.6
	r		0.12	0.14	0.18	0.23	0.21	0.18	0.14
	μ		0.07	0.11	0.17	0.15	014	0.11	0.10
	k		1.09	1.03	0.98	1.01	0.99	0.97	0.90
	$\beta \cdot 10^{-2}$, 1/K		0.38	0.34	0.30	0.28	0.24	0.22	0.20

Table 7: Response function characteristics for mixtures 1 and 2 (for T_o=20°C).
(presented as: mix.1/mix.2)

	pressure, MPa							
property	0.1	0.25	0.5	1.0	2.0	5.0	8.0	10
$Re\{U\}_m$	1.1/-	-/2.5	1.3/2.0	1.4/1.6	1.5/1.4	1.1/1.4	0.9/1.2	0.8/1.1
ω_{n1}	5.25/-	-/8.0	5.5/6.25	5.5/4.25	6.0/3.5	6.5/4.0	6.8/4.25	7.3/5.0
ϖ_{n1}, KHz	0.09/-	-/0.02	0.29/0.01	0.5/0.03	0.91/0.06	2.4/0.23	4.0/0.37	5.2/0.54
ω_{n2}	4.7/-	-/7.68	5.2/5.63	5.1/3.7	5.3/3.2	5.4/4.0	5.65/3.7	6.25/4.3
ϖ_{n2}, KHz	0.08/-	-/0.017	0.27/0.01	0.46/0.02	0.80/0.06	2.0/0.23	3.3/0.32	4.46/0.46
$Re\{U\}_{20}$	0.5/-	-/1.6	0.6/1.16	0.66/0.77	0.79/0.64	0.83/.66	0.81/0.58	0.79/0.64
$Im\{U_{m+}\}$	0.27/-	-/0.67	0.34/0.46	0.36/0.3	0.38/0.26	0.2/0.26	0.14/0.22	0.11/0.2
ω_{im1}	1.75/-	-/2.5	2.0/1.75	2.0/1.25	2.0/1.0	1.5/1.0	1.25/1.25	1.25/1.25
ϖ_{im1}, KHz	0.03/-	-/0.006	0.1/0.004	0.18/0.01	0.3/0.018	0.56/0.06	0.74/0.11	0.9/0.14
$-Im\{U_{m-}\}$	-/-	-/-	0.5/0.7	0.6/0.6	0.65/0.5	-/0.5	-/0.4	-/0.4
ω_{im2}	-/-	-/-	15/21.5	15/16	17/13	-/14.5	-/16.5	-/22.5
ϖ_{im2}, KHz	-/-	-/-	0.78/0.05	1.3/0.1	2.6/0.24	-/0.8	-/1.45	-/2.43

Conclusions

The obtained peculiarities of mixture PUNE/(CL-20), (30:70), combustion, at T_o=20°C, in comparison with those of mixture PUNE/HMX, (30:70), are as follows:

a significant carbon residue on the burning surface at pressures up to about 2 MPa (mixture 2 has no carbon residue);

significantly higher burning rates, than burning rates of mixture 2; burning rate pressure sensitivities are lower and burning rate temperature sensitivities are higher than those of mixtute 2.

significantly lower burning surface temperatures, than those for mixture 2; surface temperature sensitivities to pressure and to initial temperature are also lower than those for mixture 2 (at p>2 MPa);

heat release in solid for mixture1 is significantly lower than that for mixture 2; heat release rate in gas close to the burning surface for mixture1 is significantly higher than that for mixture 2;

activation energy of solid gasifications in combustion waves is equal to 34 Kcal/mole for mixture 1 (it is equal to 24 Kcal/mole for mixture 2 in studied pressure interval);

both systems, mixtures 1 and 2, burn steady, have two-zone structure of the gas phase (at pressures up to 3-5 MPa), burning rate control for both systems performs thin solid reaction layer on the burning surface and thin low-temperature gas layer close to the surface;

both systems, mixtures 1 and 2, have resonance phenomena in field of pressure pulsations, which are significantly depressed due to viscous behaviour of the burning rate oscillations; mixture 1 has lower amplitude of response functions, than those of mixture 2; absolute values of cyclic resonance frequencies for mixture 1 approximately an order higher than those for mixture 2.

6. Preliminary results for mixture (BAMO-AMMO)/HNIW, 20:80.

Mixtures (BAMO-AMMO)/CL-20, 20:80, were prepared in the end of this work.
Sum formula: $O_{23.9}H_{33.05}N_{26.95}C_{17.21}$; sample density ρ=1,75 g/cm^3, T_{ad}=3200 K (at 10 MPa).
Burning rates were obtained during preliminary measurements at T_o=20°C. Mass burning rates were as follows: 0.6, 2.0 and 5.0 g/cm^{2}s at pressures 0.5, 2.0 and 5.0 MPa, correspondingly. Preliminary measurements of temperature profiles show, that gas phase of the combustion waves has two-zone structure. The mesurements are continued.

Recommendations

In future work must be investigate in detail peculiarities of combustion mechanisms of mixtures on the base of CL-20, with active binders GAP, (AMMO-BAMO), THF, and at optimal ratio of oxidizer/binder (close to 80:20). The investigations at different pressures and initial temperatures allow characteristics of the mixture combustion at stable pressure and at significant pressure pulsations to be found.

FIGURES

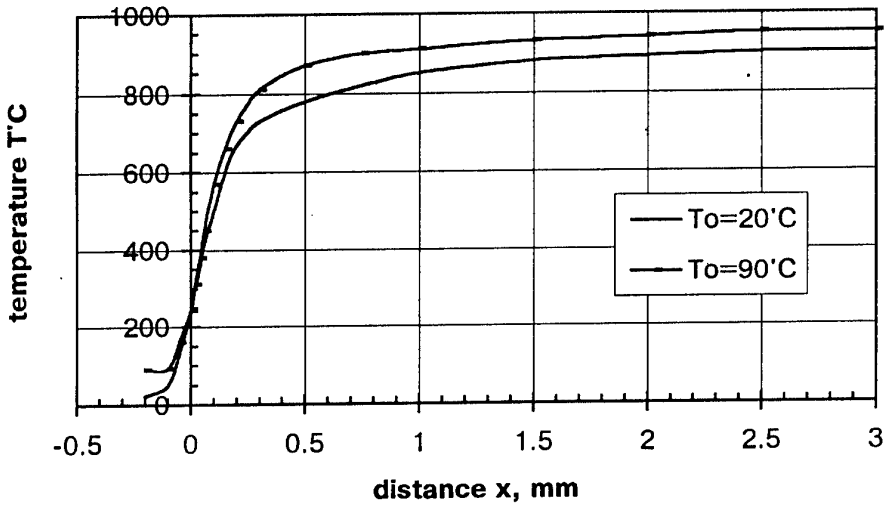

Figure 1: Averaged temperature profiles of mixt.1 at 0.1 MPa and various To.

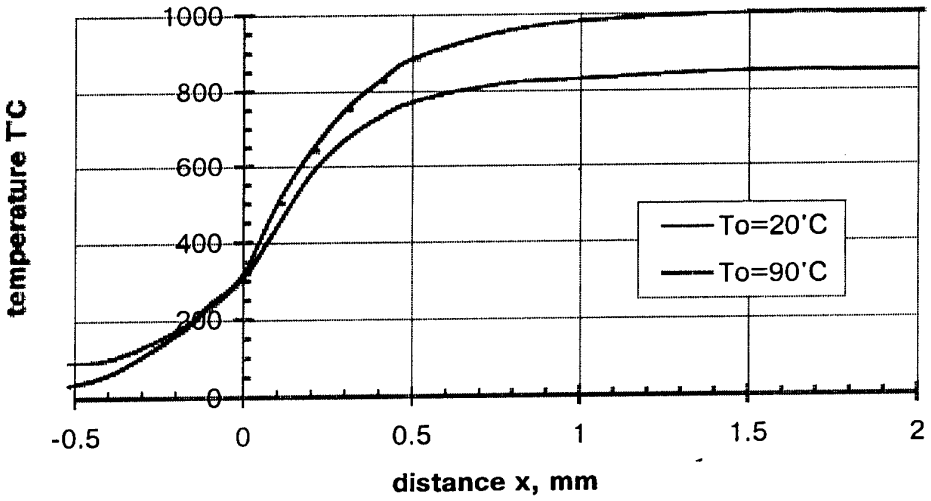

Figure 2: Averaged temperature profiles of mixt.2 at 0.25 MPa and various To.

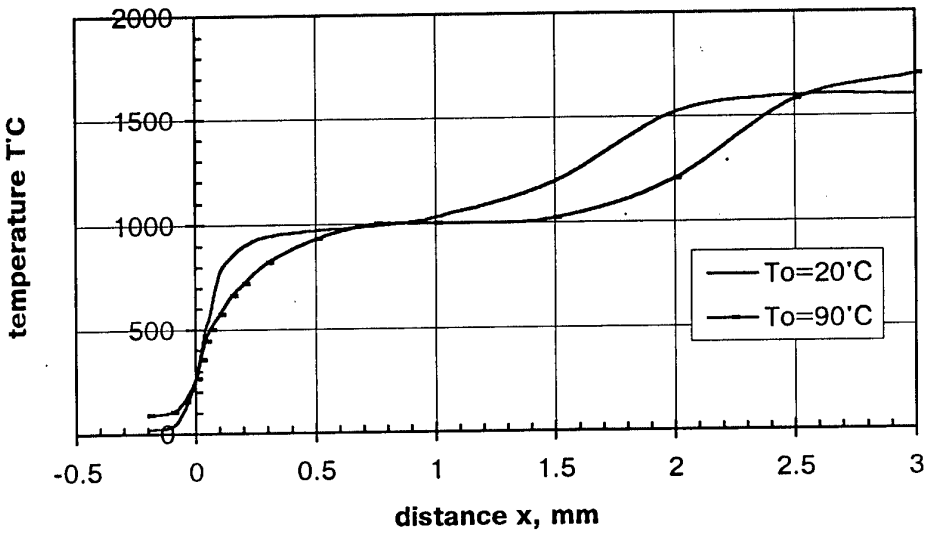

Figure 3: Averaged temperature profiles of mixt.1 at 0.5 MPa and various To.

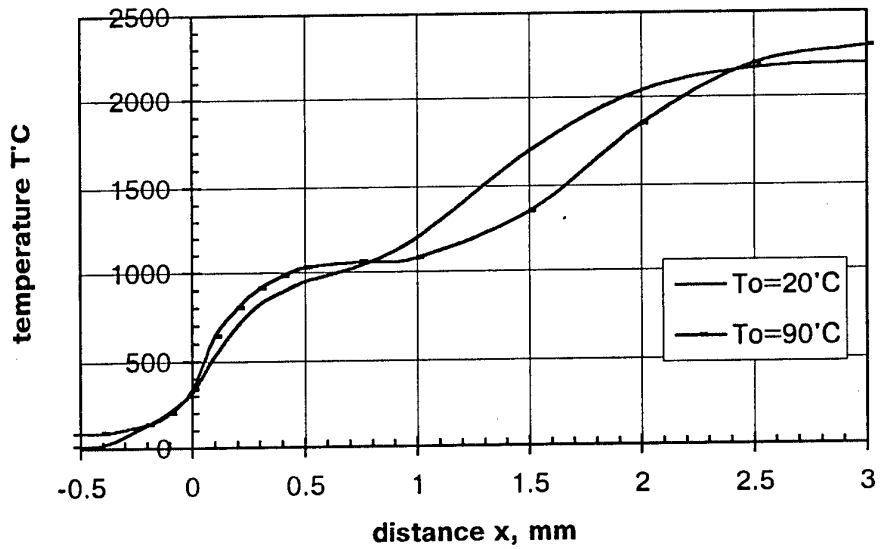

Figure 4: Averaged temperature profiles of mixt.2 at 0.5 MPa and various To.

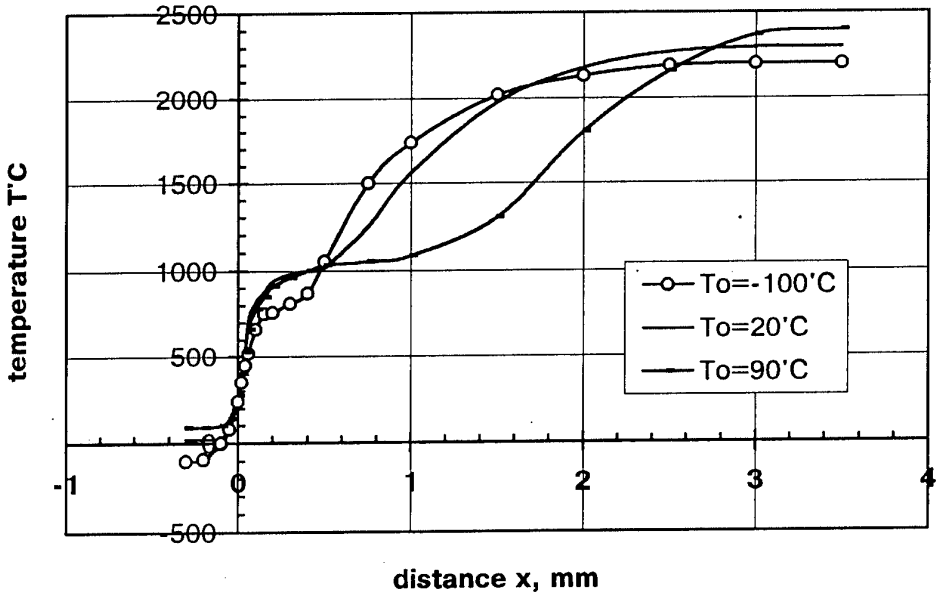

Figure 5: Averaged temperature profiles of mixt.1 at 1 MPa and various To.

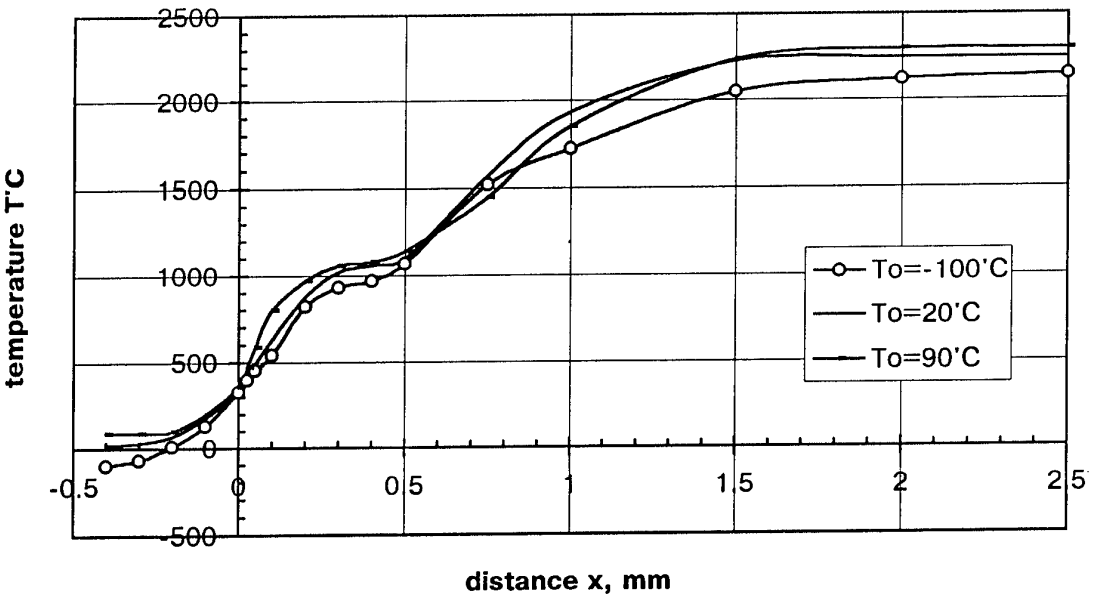

Figure 6: Averaged temperature profiles of mixt.2 at 1 MPa and various To.

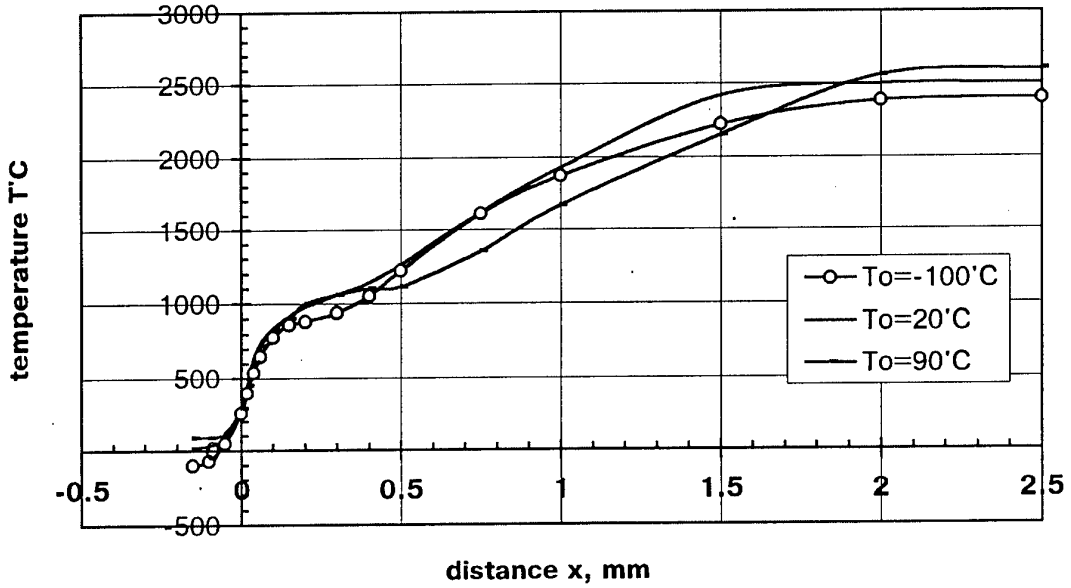

Figure 7: Averaged temperature profiles of mixt.1 at 2 MPa and various To.

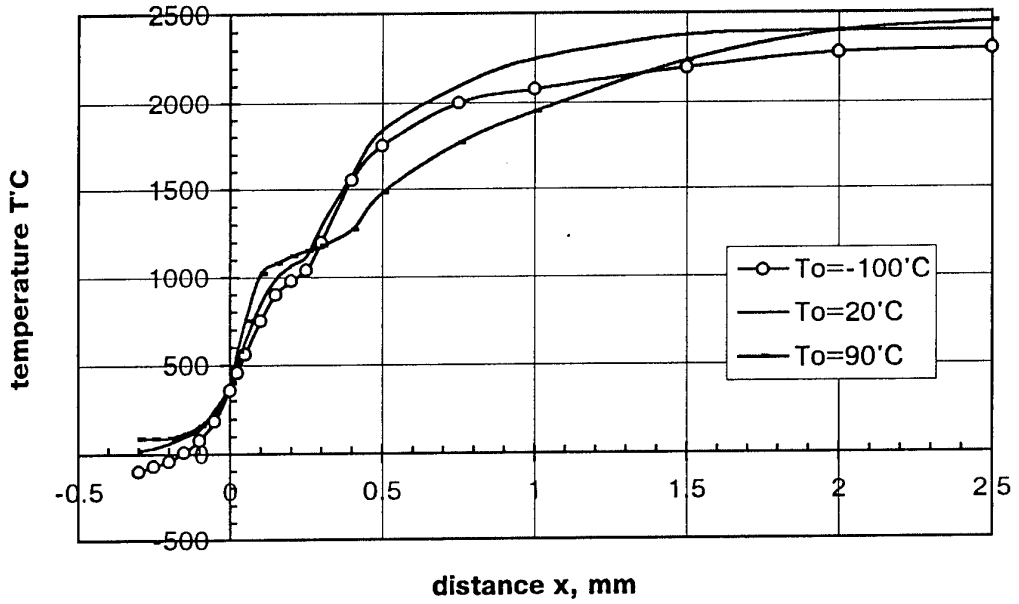

Figure 8: Averaged temperature profiles of mixt.2 at 2 MPa and various To.

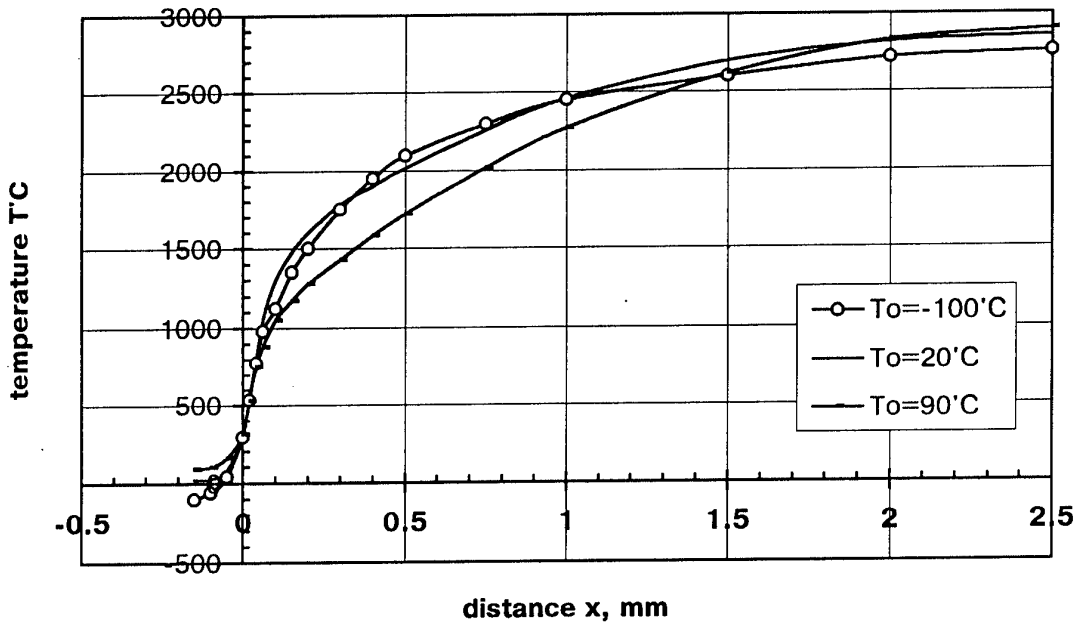

Figure 9: Averaged temperature profiles of mixt.1 at 5 MPa and various To.

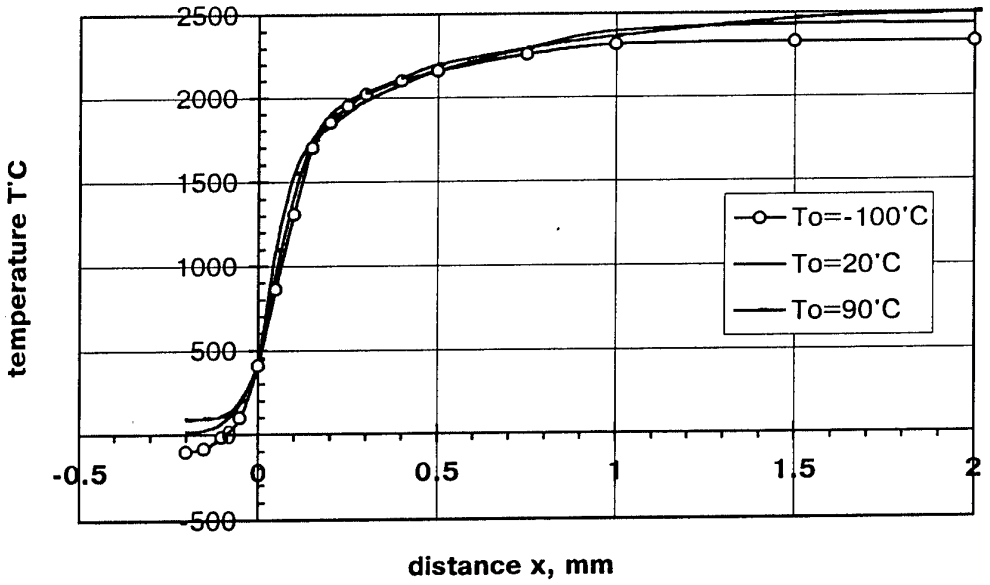

Figure 10: Averaged temperature profiles of mixt.2 at 5 MPa and various To.

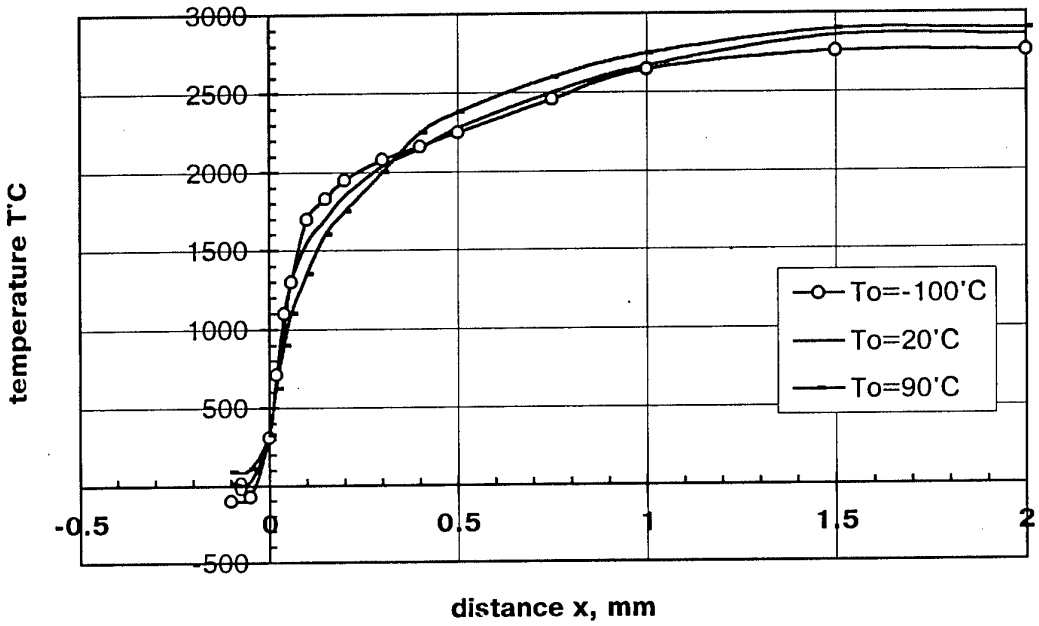

Figure 11: Averaged temperature profiles of mixt.1 at 10 MPa and various To.

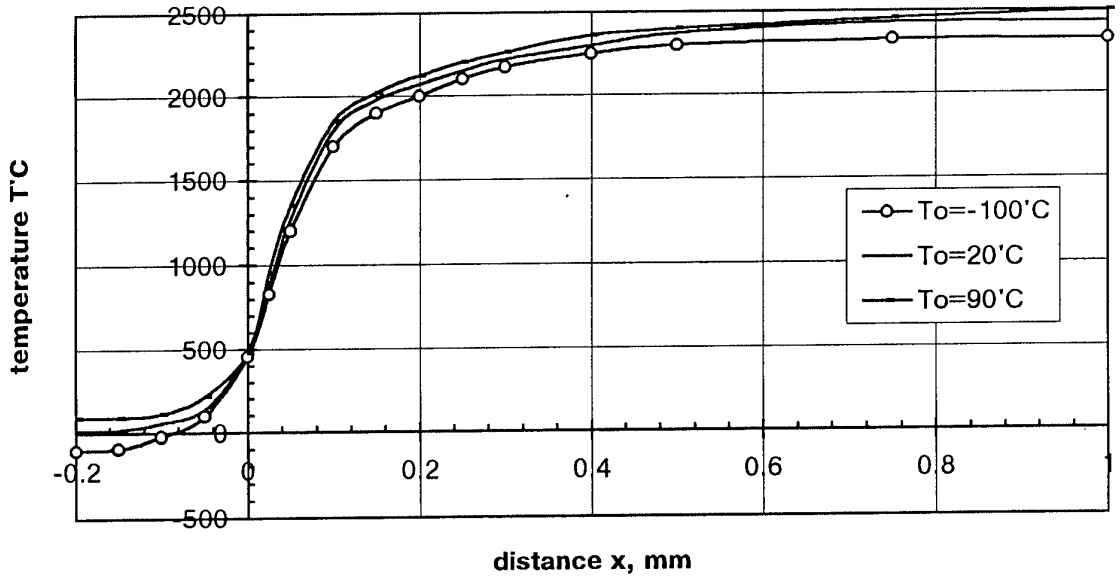

Figure 12: Averaged temperature profiles of mixt.2 at 10 MPa and various To.

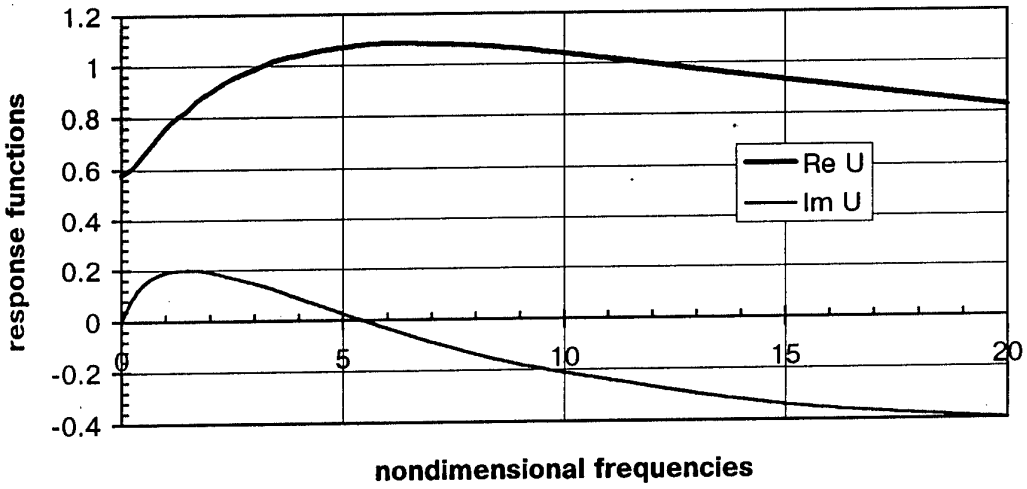

Figure 13: Typical response functions Re U and Im U for mixture 1 (5 MPa, To=20'C)

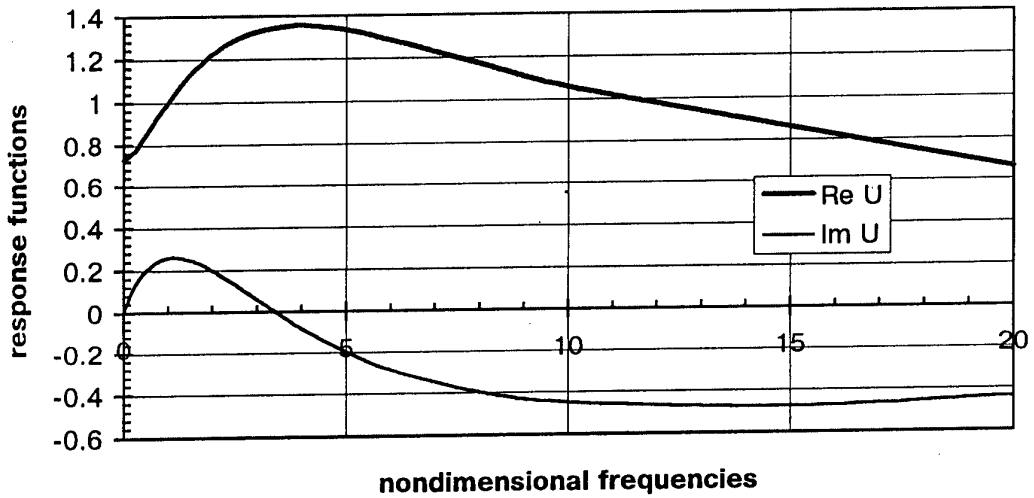

Figure 14: Typical response functions Re U and Im U for mixture 2 (5 MPa, To=20'C)